Polymorphism in Poly(diethylphosphazene) and Its Cyclic Trimer: A MAS NMR and X-ray Diffraction Study

Stefano V. Meille* and Alessandra Farina

Dipartimento di Chimica, Politecnico di Milano, Via Mancinelli 7, 20131 Milano, Italy

Maria C. Gallazzi

Dipartimento di Chimica Industriale, Politecnico di Milano, Piazza L. da Vinci 32, 20133 Milano, Italy

Piero Sozzani,* Roberto Simonutti, and Angiolina Comotti

Centro NMR dello Stato Solido, Istituto Ronzoni e Università di Milano, via Colombo 81, 20133 Milano, Italy

Received August 8, 1994; Revised Manuscript Received October 27, 1994®

ABSTRACT: Poly(diethylphosphazene) (PDEP), contrary to other polyphosphazenes, is hardly soluble in standard organic solvents and presents a melting point 80 °C higher than that of the dimethyl analog. Stimulated by this specificity, we have investigated the polymorphic behavior of PDEP and its cyclic trimer by X-ray diffraction, MAS NMR, and differential scanning calorimetry. The crystal structure of the native room temperature form of the cyclic trimer has been solved. The resulting arrangement of the ethyl groups has provided the basis to interpret the MAS NMR spectra of the trimer itself and of the polymer in the native modification, which present remarkable similarities. The MAS NMR data show analogous averaging of the ethyl side-chain conformations in the modifications obtained heating samples above the transition temperature of both the trimer and the polymer. X-ray and thermal data indicate that extensive tridimensional order must be maintained in these forms. Both modifications of PDEP obtained after thermal treatment present very significant side-chain mobility, coupled, in one of them, with only minor perturbations of the main-chain conformation and of the packing as compared to the native form. These unusual features imply for the disordered phases of PDEP a model substantially differing from the hitherto reported polyphosphazenic mesophases, which may account for the specificity of crystalline PDEP.

Introduction

Like siloxanes, polyphosphazenes (Figure 1) are macromolecules with an inorganic backbone structure which, however, consists of alternating phosphorus and nitrogen atoms. Poly(dichlorophosphazene) can be considered the precursor of this class of polymers. By substitution of the chlorine atoms in the polymer with alkoxy or aryloxy groups, a large variety of different macromolecular systems has been obtained.[1]

Diphenoxy-substituted polyphosphazenes are among the most studied and exhibit two first-order transition temperatures.[2-9] The lower one, denoted as $T(1)$, appears to involve transformation from a crystalline to a mesomorphic phase generally characterized by a single diffraction peak, related to the interchain distance in a hexagonal packing. These mesophases are commonly characterized by substantial mobility of the side chains, leading to a very disordered conformation of the flexible backbone structure. The upper transition, T_m, corresponds to the mesomorphic to isotropic transition and has usually a very low ΔH_m value, as most of the disordering is achieved at $T(1)$. Because of this and due to thermal degradation often occurring at lower temperature, T_m is often hardly detectable. Analogous behavior is shown by poly[bis(trifluoroethoxy)phosphazene],[10-12] while new data are available for other alkoxy-substituted systems.[13,14]

Recently, alkyl-substituted polyphosphazenes have been synthesized by condensation of the corresponding *N*-silylphosphoranimine.[15] While poly(dimethylphosphazene) (PDMP) has been characterized crystallographically and as far as the thermal behavior,[16-18] very limited data are available on poly(diethylphosphazene) (PDEP). These two polymers, apparently very similar, show large differences in thermal and solubility behavior. PDMP presents only the melting transition at 145 °C and it is soluble in both polar and apolar solvents. On the contrary PDEP exhibits a first-order transition at 45 °C and the melting transition at 230 °C, more than 80 °C higher than PDMP. Moreover, PDEP is quite insoluble in most common solvents. We decided therefore to investigate the solid-state behavior of PDEP, which substantially differs from both PDMP and other previously studied polyphosphazenes.

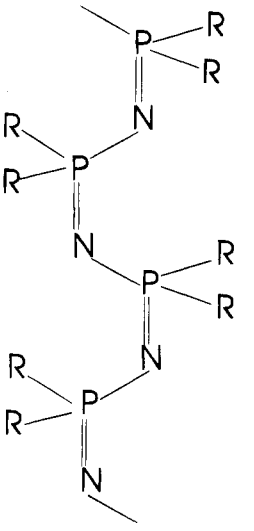

Figure 1. General structural scheme of polyphosphazenes.

® Abstract published in *Advance ACS Abstracts,* January 1, 1995.

0024-9297/95/2228-1893$09.00/0

In the present paper a first interpretation of the solid-state phenomena occurring in PDEP will be attempted. A parallel study was carried out on the cyclic trimer (TDEP), which turned out to be a reliable model for PDEP.

Experimental Section

Synthesis. Poly(dimethylphosphazene) (PDMP) was prepared and characterized as previously reported.[19] Typical values of M_n were around 40 000.

Poly(diethylphosphazene) (PDEP). The monomer $Me_3SiN{=}P(OCH_2CF_3)Et_2$ was prepared following the procedure described for the methyl derivative. Boiling points and ^{31}P NMR (H_3PO_4 external standard) chemical shifts of the synthesis intermediates are reported hereafter: *P,P*-diethyl-*N,N*-bis(trimethylsilyl)phosphinous amide, bp = 67 °C (0.2 mm), δ = 57.4; *P,P*-dimethyl-*N*-(trimethylsilyl)phosphorimide bromide, bp = 62 °C (0.3 mm), δ = 32.4; 2,2,2-trifluoroethyl *P,P*-diethyl-*N*-(trimethylsilyl)phosphorimidate, bp = 53 °C (0.3 mm), δ = 41.4. PDEP was obtained by heating 10–20 mL of the monomer in a thick-wall glass vial sealed in vacuum in an oven at 190 °C for 4 days. After cooling to room temperature the vial was opened and immediately connected to a vacuum pump to eliminate $Me_3SiOCH_2CF_3$ and the residual monomer. Then the polymer was washed with methanol and hexane and dried at reduced pressure (found, C, 46.10; H, 9.85; N, 13.20; calcd, C, 46.59; H, 9.77; N, 13.58). Yield 60%. Due to solubility problems it was impossible to determine the molecular mass of PDEP. We can expect, however, values not substantially different from those found for PDMP.

Hexaethylcyclotriphosphazene (TDEP). A four milliliter sample (4.8 g) of $Me_3SiN{=}PBrEt_2$ was sealed in a glass tube and heated in an oven at 200 °C for 40 h. After cooling, the vial was opened and kept at reduced pressure to eliminate Me_3SiBr. The residue was sublimed at 60 °C (0.1 mmHg) and consisted of a mixture of 90% trimer and 10% tetramer (^{31}P NMR (D_2O): δ 41.29 (trimer), 38.45 (tetramer)). Yield 70%. Pure trimer was obtained by two successive recrystallizations from hexane. Melting point, 118–119 °C (lit. mp 110–114[20] and 117.5–119 °C[21]).

Calorimetry. DSC runs were carried out using a Perkin-Elmer DSC-7 differential scanning calorimeter equipped with a CCA-7 liquid nitrogen cooling device. Polymer and trimer samples were studied respectively in the range 10–250 and 10–140 °C. Typical heating and cooling rates were 10 °C/min.

X-ray Diffraction. X-ray investigations of the polymer were carried out on powder samples with an Italstructures θ/θ diffractometer equipped with a thermostatic control system using nickel-filtered Cu Kα radiation. Powder diffraction patterns of the trimer were obtained with a Debye camera in vacuum due to the limited quantities of sample available.

The study of TDEP was carried out on single crystals obtained by recrystallization from hexane at 0 °C. A Philips PW1100 diffractometer was used, with graphite-monochromated Cu Kα radiation, at 25 °C.

NMR Analysis. High-resolution ^{13}C MAS NMR spectra were run at 75.5 MHz on a CXP300 Bruker instrument operating at a static field of 7.4 T. A Bruker magic angle spinning probe was used with 7 mm ZrO_2 rotors spinning at a standard speed of 5 kHz. Cross-polarization spectra were collected with contact times of 2.8 ms; MAS experiments without cross polarization were performed with a 90° pulse of 3.5 μs. High-power proton decoupling (DD) of 15 G was applied. The delay between pulses was 4 s for CP MAS and 8 s for MAS. CP MAS and MAS experiments were performed at different temperatures from 293 to 383 K. For each spectrum 400–1000 transients were collected. The best resolution was achieved with acquisition times of 55 ms and spectral widths of 11 kHz. Relaxation measurements of ^{13}C T_1 were performed by inversion–recovery and Torchia methods,[22] and for each measurement more than 12 experiments were run. ^1H $T_{1\rho}$ relaxation times were indirectly measured through ^{13}C resonances by methods described elsewhere.[23] The resolution was checked on glycine (width at half-height = 26 Hz). Crystalline polyethylene (PE) was used as an external reference at 33.63 ppm from tetramethylsilane (TMS). Chemical shift corrections with temperature were applied; PE spectra were run before and after each experiment.

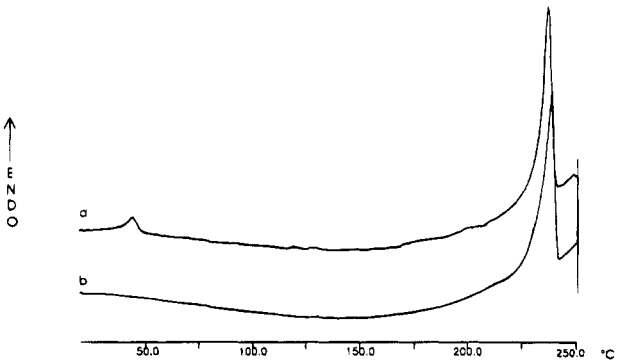

Figure 2. DSC of poly(diethylphosphazene) (PDEP): (a) native sample; (b) second heating.

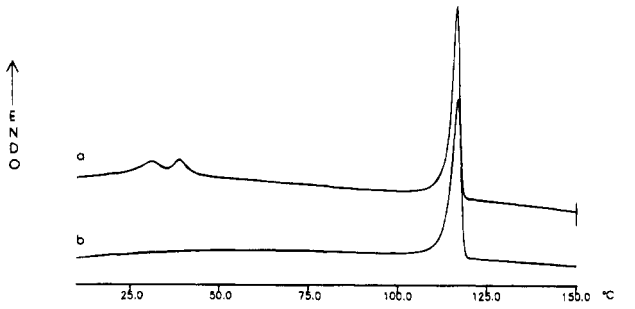

Figure 3. DSC of the cyclic trimer of diethylphosphazene (TDEP): (a) native sample; (b) second heating.

Results and Discussion

Thermal Behavior. DSC runs, as performed starting from −100 °C, do not show any clear indication of the glass transition. This is consistent with the high crystallinity of the samples and with literature reports.[15] As-polymerized PDEP (hereafter called "native" PDEP) shows a reversible thermal transition at 45 °C and the melting endotherm at 230 °C, which compares well with the literature melting point[15] (Figure 2a). The second run obtained after cooling at 5 K/min from the melt is also reported (Figure 2b). After this treatment the transition at 45 °C disappears in successive heating cycles whereas the melting temperature and enthalpy remain nearly constant.

The cyclic trimer (TDEP) shows a similar thermal behavior: the first heating scan presents a double peak at 30–40 °C and the melting endotherm at 117 °C (Figure 3a). In this case the transition is not reversible if the temperature exceeds 40 °C. Representative heating scans of samples recrystallized from the melt are reported in Figure 3b.

It appears important to note that for both the polymer and the trimer the heat involved in the low-temperature transition is only a small fraction of the isotropization enthalpy. Such a behavior is essentially the opposite of what is normally found in polyphosphazenes with two first-order transitions[1] and suggests that the high-temperature modifications in the present case preserve a higher degree of order than the typical polyphosphazene mesophases.

Dry PDMP does not show any transition in the range from 10 °C to the melting point. A broad endotherm may occur around 70–90 °C and is related to the presence of water and the occurrence of a hydrated structure.[17] The enthalpies measured for the melting

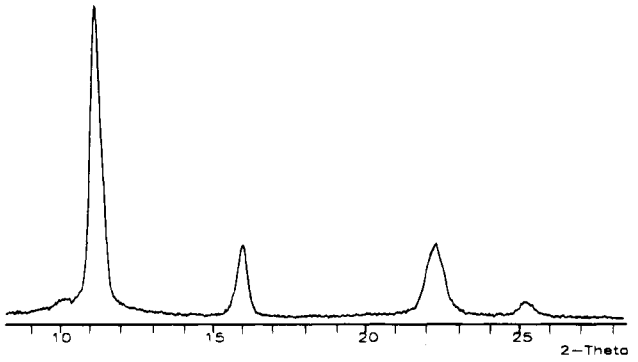

Figure 4. X-ray diffraction pattern (Cu Kα) of native PDEP (form I).

Table 1. Melting Temperatures, Enthalpies, and Calculated Entropies for PDEP and PDMP

	T_m (°C)	ΔH_m (kJ/mol)	ΔS_m (J/(mol K))
PDEP	230	7.0	14
PDMP	143	5.5	13

transitions of the two polymers and the calculated entropies are reported in Table 1.

Solution NMR Characterization. PDEP was found to be soluble only in protonating solvents; therefore solution NMR spectra were performed in DCOOD. ^{31}P spectra were recorded to check the purity of the polymer and of the cyclic trimer.

The ^{13}C NMR spectrum of PDEP, being decoupled from hydrogen, shows a simple pattern containing the coupling to ^{31}P nuclei. Due to the distance existing between the coupled nuclei the $^{31}P-^{13}C$ coupling is larger on methylenes than on methyls, i.e., respectively 82 and 5 Hz. These values will be later useful for the interpretation of the MAS NMR data.

Hydrogen spectra of PDEP were collected at different magnetic fields. Patterns are dominated by the couplings between ^{1}H and ^{31}P and between hydrogens, both being abundant nuclei. This is demonstrated by the values of the splittings at different magnetic fields (80 and 200 MHz) which are directly proportional to the H_0 magnetic field. The coupling constants of hydrogens with ^{31}P are larger on methyls than on methylenes. Similar spectra, but with slightly different chemical shifts, characterize also TDEP. In the fast-motion regime, characteristic of dissolved samples, all ethyl groups are equivalent. On the contrary, conformational differences among ethyl groups are apparent from the solid-state NMR data.

PDEP Characterization by X-ray Diffraction. PDEP could not be oriented, probably due to the rather low molecular weight, and thus the X-ray characterization is limited to powder data. Powder diffraction patterns of PDEP were obtained from native samples at different temperatures (20–100 °C). As no significant differences are observed, except for the expected lattice expansion, in Figure 4 only the room temperature profile is reported. The virtual independence of the diffraction pattern from temperature is quite surprising considering the thermal behavior resulting from the DSC investigation, showing a transition around 45 °C. However, since we can expect the main features of X-ray scattering by PDEP to result from the position of the phosphorus atoms, modification of side-group conformations may be undetectable if the original main-chain conformation and the crystal packing are maintained. This may be true especially if different modes (static vs dynamic) or different degrees of side-chain disorder are involved in the two phases, as later discussed.

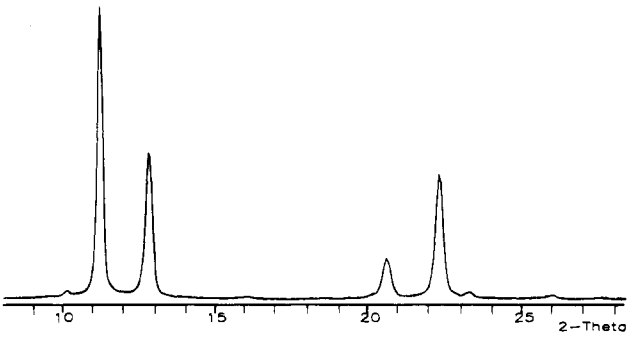

Figure 5. X-ray diffraction pattern (Cu Kα) of PDEP recrystallized from the melt (form II).

Table 2. Main X-ray Diffraction Reflections (Cu Kα) of the Two Crystalline Forms of PDEP

form I		form II	
2θ (deg)	int	2θ (deg)	int
10.0	m	10.0	m
11.0	vs	11.2	vs
		12.6	s
14.4	mw		
16.0	s		
20.0	mw		
		20.4	ms
22.2	s	22.2	s
		23.1	mw
25.4	m	25.4	mw
29.8	w	29.8	w
		30.8	w
32.6	w	32.6	w
33.8	w		
		34.1	w
35.9	w	35.9	w
41.8	w		

After melting and recrystallization, samples showing different profiles were obtained, suggesting the existence of a different crystalline polymorph (form II) of PDEP, which can coexist with the native crystalline phase (form I). Crystallization close to the melting point (225 °C) affords essentially pure form II (Figure 5), while at lower temperatures variable proportions of the two phases result. Form I and form II appear to have very similar melting temperatures and enthalpies and can hardly be distinguished by DSC. The main diffraction maxima of the two polymorphs are listed in Table 2. Preliminary indexing attempts suggest that both crystalline forms are compatible with the typical phosphazene axial periodicity of 4.9 Å or multiples thereof. The most probable chain conformation is thus the same adopted by PDMP, the nearly *cis–trans* planar conformation, as later discussed in connection with the MAS NMR spectra.

Hardly any amorphous contribution is apparent in the diffraction patterns of both phases, which are, as already noted,[15] highly crystalline. More specifically, neither displays the features of typical polyphosphazene mesophases which present a single very intense diffraction maximum related to the interchain distance. On the contrary, both modifications of PDEP are characterized by many intense diffraction peaks occurring also at relatively high angle and suggesting a considerable degree of tridimensional order.

TDEP Characterization by X-ray Diffraction. The crystal structure of the cyclic oligomer (TDEP) was determined from single-crystal data. Crystal data are as follows: $N_3P_3C_{12}H_{30}$, MW = 309.30, monoclinic, a =

Table 3. Atomic Coordinates ($\times 10^4$) and Equivalent Isotropic Displacement Parameters ($Å^2 \times 10^3$) of TDEP

atom	x	y	z	U(eq)[a]
P(1)	1154 (3)	2500	4598 (4)	90 (1)
P(2)	−1421 (2)	1480 (1)	5275 (3)	84 (1)
N(1)	−2336 (8)	2500	5317 (9)	80 (2)
N(2)	267 (6)	1509 (3)	4814 (7)	87 (2)
C(11)	3445 (11)	2500	5981 (16)	118 (4)
C(12)	3759 (13)	2500	7803 (14)	139 (5)
C(13)	1133 (18)	2500	2436 (16)	148 (5)
C(14)	2078 (24)	3072 (12)	2002 (23)	159 (8)
C(21)	−3025 (10)	673 (5)	3862 (11)	112 (3)
C(22)	−3657 (11)	960 (7)	2072 (11)	142 (3)
C(23)	−711 (9)	896 (5)	7318 (10)	110 (3)
C(24)	−2060 (11)	827 (6)	8049 (11)	150 (3)

[a] U(eq) is defined as one-third of the trace of the orthogonalized U_{ij} tensor.

Table 4. Bond Lengths and Angles of TDEP[a]

atoms	length (Å)	atoms	angle (deg)
P(1)−N(2)	1.591 (5)	N(2)*−P(1)−N(2)	117.7 (3)
P(1)−C(11)	1.784 (9)	N(2)−P(1)−C(11)	109.4 (3)
P(1)−C(13)	1.864 (12)	N(2)−P(1)−C(13)	107.3 (3)
P(2)−N(1)	1.598 (3)	C(11)−P(1)−C(13)	104.8 (6)
P(2)−N(2)	1.595 (4)	N(1)−P(2)−N(2)	116.8 (3)
P(2)−C(21)	1.781 (7)	N(1)−P(2)−C(21)	109.5 (3)
P(2)−C(23)	1.812 (7)	N(2)−P(2)−C(21)	108.9 (3)
C(11)−C(12)	1.492 (12)	N(1)−P(2)−C(23)	109.7 (3)
C(13)−C(14)	1.265 (14)	N(2)−P(2)−C(23)	106.4 (3)
C(21)−C(22)	1.476 (9)	C(21)−P(2)−C(23)	104.8 (4)
C(23)−C(24)	1.487 (10)	P(2)*−N(1)−P(2)	122.5 (4)
		P(1)−N(2)−P(2)	122.6 (3)
		C(12)−C(11)−P(1)	113.4 (7)
		C(14)−C(13)−P(1)	122.7 (12)
		C(22)−C(21)−P(2)	114.0 (6)
		C(24)−C(23)−P(2)	116.1 (5)

[a] Symmetry transformations used to generate equivalent atoms *: $x, -y + 1/2, z$.

8.239 (2) Å, b = 13.741 (9) Å, c = 8.657 (4) Å, β = 113.66 (2)°, V = 897.7 (7) Å^3, Z = 2, d_c = 1.144 g/cm^3, $F(000)$ = 336, μ = 2.954 mm^{-1}. Cu Kα radiation was used and two standard reflections were measured every 100 reflections to check the stability of the crystal and of the experimental conditions; no significant variations were detected. Of the collected 1181 independent reflections with $2 \le \theta \le 55°$ ($\pm h, +k, +l$), 565 reflections were considered observed ($I > 2\sigma(I)$). Lorentz and polarization corrections were applied, but no absorption correction. The structure was solved by direct methods using SHELXS-86[24] and refined by full-matrix least squares with SHELXL-93.[25] Hydrogen atoms were included at calculated positions and refined in the riding mode. Atomic coordinates are given in Table 3, while relevant molecular dimensions are reported in Tables 4 and 5.

Although the crystal was of rather poor quality, we were able to obtain an acceptable data set. The data collection was, however, carried out at ambient temperature, i.e., just a few degrees below the transition to form II. The relatively high values of the thermal factors for the ethyl groups are therefore not surprising. Given the limited number of observed reflections, close to the maximum allowable number of parameters (~100) were refined using the $P2_1/m$ and $P2_1$ symmetries, which are both compatible with the systematic absences. In $P2_1/m$ the molecule has a crystallographic intramolecular mirror plane that reduces the independent non-hydrogen atoms to 12 and allows consideration of the anisotropic thermal motion of the carbon atoms, using 95 parameters. With space group $P2_1$ the asymmetric unit involves a complete molecule, i.e., 18 independent atoms, of which only the phosphorus and the nitrogen could be refined anisotropically, using 104 parameters. R values of 0.069 and 0.073 were obtained respectively for the two space groups, indicating that, with the available data set, the introduction of the carbon atom anisotropy in the higher symmetry $P2_1/m$ space group yields a better model that the lower symmetry space group $P2_1$ and is therefore adopted.

Table 5. Selected Torsion Angles of TDEP[a]

atoms	angle (deg)
N(2)−P(2)−N(1)−P(2)*	−12.2 (7)
C(21)−P(2)−N(1)−P(2)*	−136.5 (5)
C(23)−P(2)−N(1)−P(2)*	109.0 (5)
(2)*−P(1)−N(2)−P(2)	−1.5 (7)
C(11)−P(1)−N(2)−P(2)	124.2 (5)
C(13)−P(1)−N(2)−P(2)	−122.6 (5)
N(1)−P(2)−N(2)−P(1)	6.6 (6)
C(21)−P(2)−N(2)−P(1)	131.3 (4)
C(23)−P(2)−N(2)−P(1)	−116.3 (4)
N(2)−P(1)−C(11)−C(12)	−65.2 (2)
C(13)−P(1)−C(11)−C(12)	180.0 (0)
N(2)*−P(1)−C(13)−C(14)	68.8 (14)
N(2)−P(1)−C(13)−C(14)	−163.8 (12)
C(11)−P(1)−C(13)−C(14)	−47.5 (13)
N(1)−P(2)−C(21)−C(22)	68.4 (7)
N(2)−P(2)−C(21)−C(22)	−60.5 (7)
C(23)−P(2)−C(21)−C(22)	−174.0 (6)
N(1)−P(2)−C(23)−C(24)	50.2 (7)
N(2)−P(2)−C(23)−C(24)	177.4 (6)
C(21)−P(2)−C(23)−C(24)	−67.3 (7)

[a] Symmetry transformations used to generate equivalent atoms *: $x, -y + 1/2, z$.

Table 6. Main X-ray Diffraction Reflections (Cu Kα) of the Two Crystalline Forms of TDEP

form I		form II	
2θ (deg)	int	2θ (deg)	int
		10.9	s
11.15	vs		
11.73	s		
12.53	ms		
12.89	s		
		12.7	vw[a]
14.10	w		
17.07	m		
		17.0	vw[a]
17.46	w		
19.21	ms		
20.70	m		
21.64	s		
		21.8	m
		22.3	s
22.71	s		
23.14	mw		
		23.2	m
25.94	m		
27.42	w		
		28.2	w[a]
30.03	mw		
32.00	w		
		33.1	mw
33.67	mw		
33.90	m		
35.04	w		
36.41	w		
38.22	w		

[a] Broad reflection.

A view of the cyclic trimer is shown in Figure 6. As expected, P−N bond distances are all equal within experimental uncertainty (Table 4). The ring is nearly planar, as for the trimer of dimethylphosphazene (TDMP),[26] which, however, presents only a noncrystallographic intramolecular mirror plane. The deviations

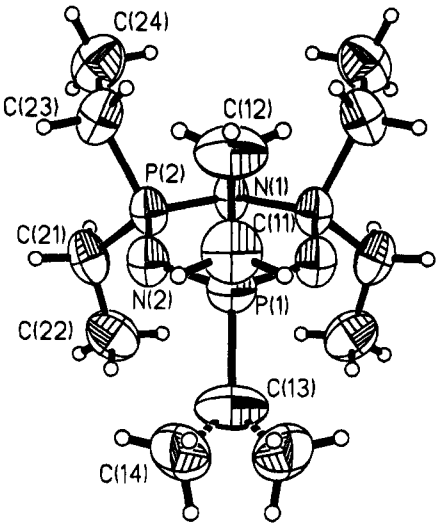

Figure 6. ORTEP view of TDEP. 30% probability thermal ellipsoids for non-hydrogen atoms are shown.

from planarity (see the torsion angles around the P–N bonds in Table 5) are somewhat less pronounced in TDEP than in TDMP.

In the $P2_1/m$ model the mirror plane is normal to the ring mean square plane and contains N(1), P(1), C(11), C(12), and C(13). The methyl carbon C(14) is disordered and has to be refined with a 0.5 occupancy factor. It is statistically present on both sides of the mirror plane and the refined C(13)–C(14) bond distance (1.265 Å) is a clear indication of the extensive conformational disorder, probably of a dynamic nature, involving this atom. On the other hand, the other carbon–carbon distances are also somewhat short, even if to a lesser degree (average 1.485), consistent with some disordering. The importance of the anisotropic treatment of the thermal motion for the ethyl groups is made apparent by the fact that the principal axes of the thermal ellipsoids of carbon atoms are oriented in directions consistent with the expected rotational disorder (Figure 6).

A different crystalline modification (form II) is obtained by recrystallizing from the melt or simply by heating the sample over 40 °C. In either case crystals suitable for single-crystal analysis could not be obtained. Debye patterns are very similar for powder samples subjected to either thermal treatment and exhibit a dramatic reduction of the number of reflections (Table 6). The measured data can tentatively be accounted for by a trigonal unit cell with $a = b = 7.95$ Å, $c = 16.24$ Å, $\gamma = 120°$, $V = 889$ Å^3, $Z = 2$, and $d_c = 1.15$ g/cm^3. If the proposed unit cell, containing two molecules, is correct and if it is truly trigonal, the molecule itself should have a threefold symmetry, suggesting that in this polymorph the three phosphorus atoms, and the corresponding side groups, are symmetry related. The high symmetry of this high-temperature form would be the result of the averaging over the different accessible conformations, i.e., of dynamic disorder, as later discussed.

MAS NMR Characterization of PDEP. In spite of the virtual identity of the X-ray diffraction spectra collected at low and high temperature for phase I, ^{13}C MAS NMR spectra show a dramatic change in the multiplicity of the signals (Figure 7). For the methyl carbons four main signals, two of them hardly resolved, were detected at room temperature (intensity pattern 1:1:1:1). This group is centered around an additional minor signal at 8.5 ppm and extends over ca. 3 ppm. At

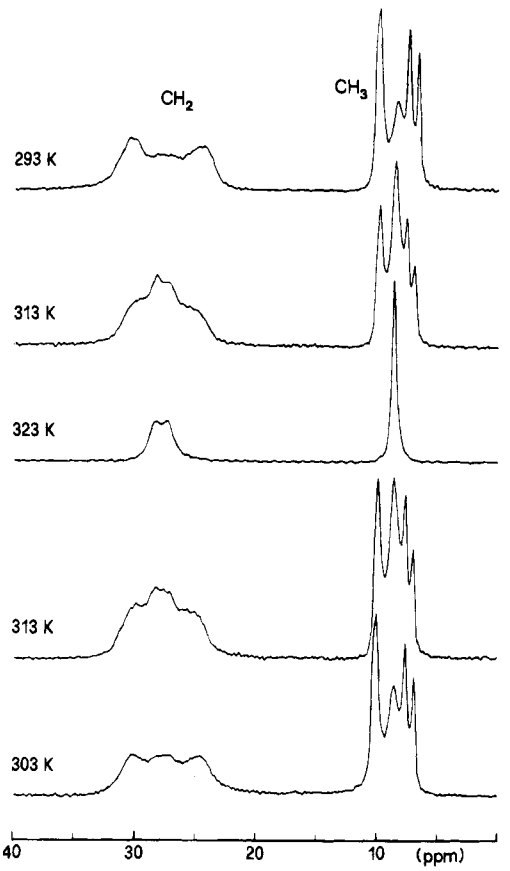

Figure 7. 75.5 MHz ^{13}C CP MAS NMR spectra of PDEP at different temperatures; a thermal cycle is presented going from 303 to 323 K and back again to 293 K.

higher temperature the NMR pattern collapses within a few degrees (40–50 °C) into the single peak at 8.5 ppm. The phase transition is reversible, consistent with the DSC results.

A similar behavior was observed for the methylene signals. However, in this case, the multiplicity of the signals coalesces into two resonances centered at about 28 ppm in the high-temperature spectrum. The splitting of 70 Hz is due to coupling to the phosphorus nucleus and retains the same value as in the solution spectrum. The splitting, although unresolved, is still present at room temperature, as will be later confirmed, and it is the reason for the broadening of the signals. Therefore, taking into account the coupling constant to ^{31}P, a single chemical shift is assigned to the methylene carbon at high temperature (Figure 7). A minor methylene signal at 28 ppm, with a behavior correlating with the minor methyl resonance at 8.5 ppm, is an additional relevant feature of the room temperature spectrum.

MAS ^{13}C NMR spectra of PDEP were collected with and without cross polarization (CP) at 5 s recycle time, showing no significant differences. This is due to the very short carbon longitudinal relaxation times that allowed us to collect MAS spectra without CP and without long recycle times. On the other hand, in spite of the short relaxation times, often indicating soft systems, our polymers can cross polarize efficiently.[27] Phosphorus and nitrogen in the partially delocalized system can contribute to the efficient relaxation of the surrounding nuclei. T_1 relaxation time measurements were run by inversion–recovery and Torchia methods[22,28] and afford values of the order of a few seconds. The assignments and the spin–lattice relaxation times T_1 are given for each signal in Table 7.

Table 7. ^{13}C Chemical Shifts and Relaxation Times for PDEP in the Different Phases[a]

	chem shift	relaxation time (s)				
		Trochia	phase I inversion–recovery		phase II inversion–recovery	
	(ppm)	293 K	293 K	323 K	293 K	323 K
CH_3	6.8	1.4	1.8			
	7.6	1.7	1.8			
	8.5	1.3	1.1	1.1	0.6	0.6
	10.0	1.7	1.9			
	10.2	1.7	1.9			
CH_2	24.3	1	1.1			
	28	0.2	0.3	0.3	0.2	0.2
	29.9	1	1.3			

[a] The estimated error on the values of the relaxation times is ±10%.

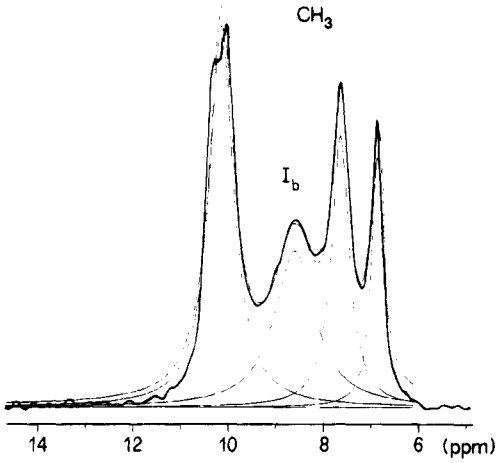

Figure 8. 75.5 MHz ^{13}C CP MAS NMR spectrum of the methyl region of PDEP at room temperature. The deconvoluted signals and the resulting calculated trace are reported for comparison.

^1H $T_{1\varrho}$ were also measured. ^1H $T_{1\varrho}$ follows the spin-diffusion phenomenon, giving an indication of the homogeneity of the sample at the nanometer scale.[29] A single value, within experimental error, was obtained for the main methyl and methylene signals at room temperature, indicating carbon atoms belonging to the same phase, while the additional minor signals, respectively at 8.5 and 28 ppm, show a different relaxation value, indicating a separate phase. These secondary low-temperature resonances occur at the same chemical shift and present the same relaxation times as the resonances in the high-temperature modification. These signals are, therefore, interpreted as due to a phase which is pure at high temperature. We refer to the phase existing in the pure form between 45 and 230 °C as phase I_b, while the remaining signals detected at room temperature are due to phase I_a. The content of modification I_b in the room temperature spectra can be estimated as about 30% (Figure 8).

Variable-temperature spectra were also recorded for modification II, but no significant change was observed in the 293–383 K range (Figure 9). The chemical shifts of phase II are not different from those observed in the high-temperature phase I_b (Figure 7 and Table 7). T_1 measurements run at the same temperature show instead a different behavior (Table 7), indicating different mobility in phase I_b and phase II, consistent with the different packing indicated by X-ray diffraction. There should be no basic differences in the polymer conformation, since in that case the effect on chemical shifts should be large enough to be detected.

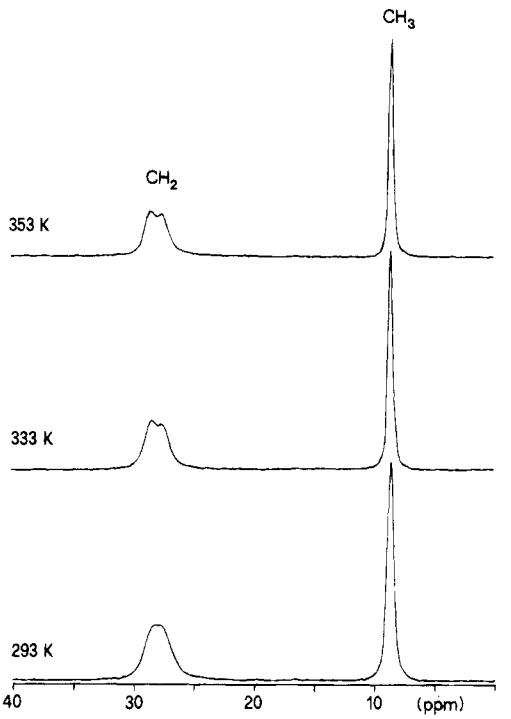

Figure 9. 75.5 MHz ^{13}C CP MAS NMR spectra of phase II of PDEP at variable temperature.

MAS NMR Characterization of TDEP. To clarify the transition involving phases I_a and I_b of PDEP, we compared the above results to those obtained characterizing the cyclic trimer of diethylphosphazene (TDEP). The ^{13}C NMR spectra recorded at increasing temperatures are reported in Figure 10. At higher temperature the spectrum simplifies, as in the case of phase I_b and phase II of PDEP. However, exceeding 30 °C by just a few degrees and approaching the 40 °C DSC transition (Figure 3), the spectra indicate that the transition is not reversible. After any treatment at temperature higher than 40 °C, the spectrum shows, when recorded at room temperature again, additional signals corresponding to the high-temperature form (Figure 10). The new signals were assigned to a phase which is referred to as form II, because, as for the polymer, phase II does not reconvert into phase I by any thermal treatment.

In particular, the methyl signals in the spectrum of TDEP appear at room temperature as a clean quartet similar to that present in PDEP. An intensity distribution following a 2:1:1:2 pattern is apparent. The chemical shift values are temperature dependent and especially sensitive when close to the transition. Specifically, the methyl range shrinks even if the resonances remain sharp; the spectrum appearance changes although the intensity distribution is not affected.

A deconvolution procedure of the CH_2 signals was performed under the assumption that a ^{31}P coupling should be present (Figure 11). High-field signals show larger J couplings (about 150 Hz) and low-field smaller J couplings (80 Hz); this is reasonable if one considers that different conformations are taken into account. By this procedure four chemical shifts (further split by coupling) were identified on the CH_2 spectrum of the trimer, as for the CH_3 spectrum. Chemical shifts and T_1 values (obtained by inversion–recovery) are reported in Table 8. The intensities of the methylene signals follow approximately the ratios 2:1:2:1, starting upfield.

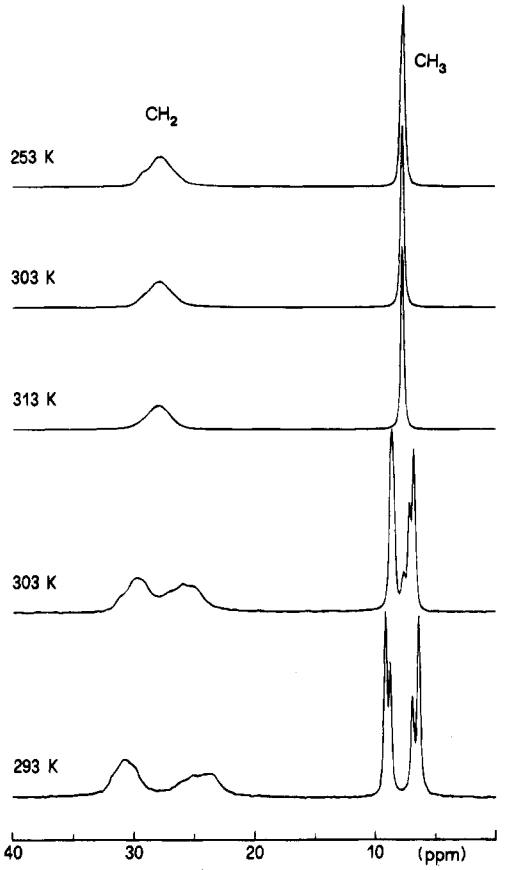

Figure 10. 75.5 MHz ^{13}C CP MAS NMR spectra of TDEP at different temperatures; a thermal cycle is presented going from 293 (lower spectrum) to 313 K and back again to 293 K (upper spectrum).

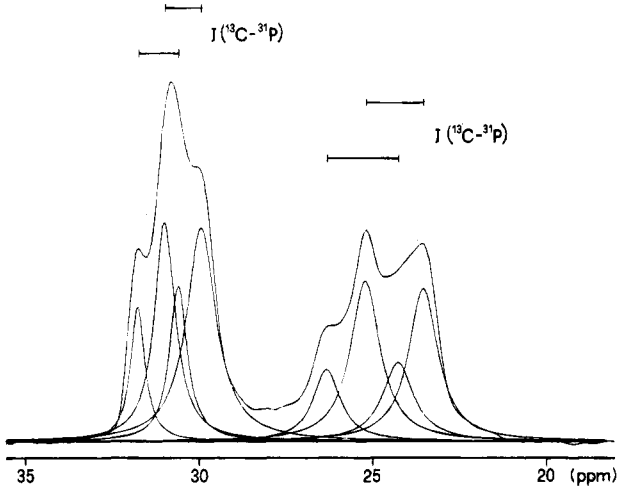

Figure 11. 75.5 MHz ^{13}C MAS NMR spectrum of the methylene region of TDEP at room temperature. The signals obtained by a deconvolution procedure are reported. $^{13}C-^{31}P$ J couplings are indicated.

The average chemical shift of the methyls is 0.8 ppm downfield for the polymer as compared to the trimer. This shift may be caused by different packing environments of the molecules. Thus the very slight differences resulting from the comparison of the two sets of chemical shifts (Tables 7 and 8) suggest that the ethyl groups in PDEP and in TDEP adopt virtually the same conformations.

MAS NMR Characterization of PDMP. The landscape is completed by ^{13}C MAS PDMP spectra (Figure 12). No transitions can be detected in the 25–120 °C range. The CH_3 linked to the phosphorus atom presents an 80 Hz J coupling to the ^{31}P nucleus and was deconvoluted, showing a pattern similar to either of the two groups of CH_2 signals (see Figure 11) of the TDEP trimer. The center of the doublets shows two chemical shifts (CSs) (24.1 and 25.2 ppm). The ratio between the signals is consistent with the published X-ray diffraction structure.[16] T_1 ^{13}C relaxation measurements were equal to 0.5 s.

Table 8. ^{13}C Chemical Shifts, Intensities, and Relaxation Times for TDEP at Room Temperature

	chem shift (ppm)	area 293 K	^{13}C T_1 (s) 293 K
CH_3	6.5	1.9	2.2
	7.0	1.1	2.2
	7.6		1.3
	8.8	1.2	1.3
	9.2	1.8	1.3
CH_2	24.4	2.2	nd
	25.3	0.6	nd
	30.5	2.2	nd
	31.2	1.0	nd

[a] The estimated error on the values of the relaxation times is ±10%.

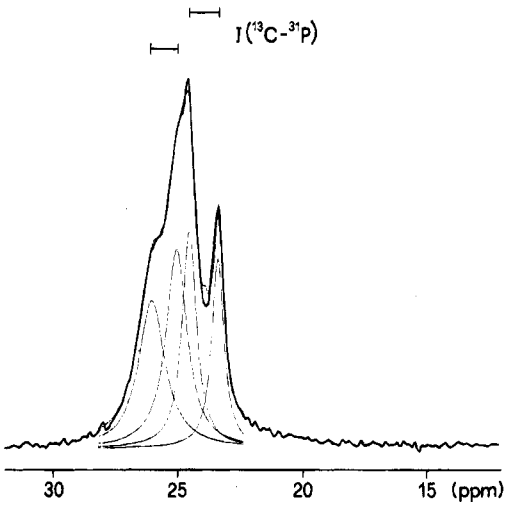

Figure 12. 75.5 MHz ^{13}C CP MAS NMR spectrum of the methyl region of PDMP at room temperature. Signals obtained by a deconvolution procedure are reported. $^{13}C-^{31}P$ J couplings are indicated.

Conformational Arrangement in the Native Polymorphs (I_a). Among the crystalline polyphosphazenes, by far the most common chain conformation is the *cis–trans* planar with an axial periodicity of 4.9 Å.[16,30,31] We can expect that this conformation is adopted also by PDEP. In fact, powder diffraction data seem compatible with such an axial periodicity, and the strong analogies between the methylene signals of PDEP and the methyl signals of PDMP in the MAS NMR spectra are evidence of a similar chain conformation, which for PDMP was established by X-ray diffraction.[16] The analogy of the MAS NMR pattern of PDEP and TDEP indicates that also for the ethyl groups similar conformations occur. This is understandable in terms of the *cis–trans* conformation adopted by the polymer which causes the local conformational environment of the alkyl side chains to be similar to that of the trimer.

Since the conformations of the ethyl groups in the trimer represent a good model for the conformation of the side chains in PDEP, they will be discussed in detail. X-ray diffraction of TDEP in form I_a shows at room temperature the ethyl groups adopting four conforma-

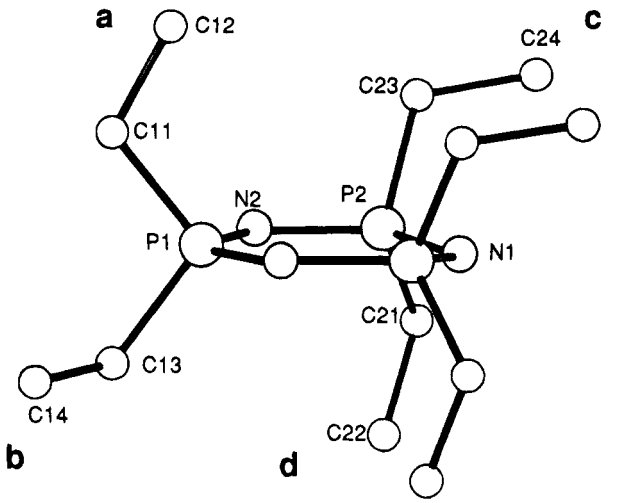

Figure 13. An arbitrary view of TDEP displaying the different ethyl group conformations.

tions, labeled **a**, **b**, **c**, and **d** (Figure 13). In conformations **a** and **d** the methyl is *trans* with respect to the methylene of the second ethyl group; it is directed toward the center of the ring and presents *gauche* interactions with two nitrogen atoms (**A**, Figure 14). In **b** and **c** conformers the methyl points toward the periphery of the ring and is *trans* to one of the N atoms and *gauche* respectively to a methylene and another nitrogen (**B**, Figure 14). The values of the corresponding torsion angles (see Table 5) suggest that, as expected, the interaction with nitrogen is more favorable (smaller torsion angles) than the one with methylene. The torsion angles involving C(14) represent an exception, and their values must be considered critically as they are probably the result of a rather crude description of disorder. Taking into account the distortion of the ring, the conformation adopted by TDEP in the crystal (see Figure 13) can be rationalized if we assume that **A** conformations are more favorable but, in order to place two ethyls in the **A** conformation on the same side of the ring, distortions result, which make it unfavorable to adopt the **A** conformation by more than one ethyl on the opposite side.

From the NMR point of view, the chemical shifts of *native* PDEP (form I_a) and TDEP (form I) at room temperature can be described in both the cases of methyls and methylenes as presenting a major splitting (about 3 ppm for CH_3 and 5–6 ppm for CH_2) and a minor one (0.5 and 1 ppm, respectively). The main factor affecting the CSs is in this case represented by γ-gauche interactions.[32] The value of the interaction depends on the dihedral angle associated with the rotation about the next neighbor bond to the observed nucleus. To find the magnitude of the chemical shift, an interaction will be defined generically as *gauche* (G) for dihedral angles in the 52.5–67.5° range. *Strong* interactions (G_s) and *weak* interactions (G_w) are defined when respectively smaller and larger angles are explored. A further specification is due to the fact that the interaction may involve nitrogen (G_N) or carbon (G_C) atoms. The methylene carbons are conveniently described by two interaction parameters and will be thus discussed before methyls. On the other hand, the methylene spectrum is not immediately understandable because it contains the splittings due to ^{31}P couplings. Each group of methylene signals in the spectrum shows an analogy to the ^{13}C spectrum of PDMP (Figure 12), which is due to methyls directly linked to the phosphorus atom. Note that no carbon–carbon γ-*gauche* interactions can occur in the case of PDMP. The carbon–carbon γ-*gauche* interactions are, therefore, responsible for the existence of two groups of signals in the PDEP and TDEP spectra, centered about 5 ppm apart. The deconvolution already presented in Figure 11 evidences the coupling to ^{31}P and the chemical shift values of the carbon atoms (Table 8).

The interactions occurring in TDEP can be indexed in the following way (still refer to Figures 13 and 14). The labels indicate the ethyl group of the observed methylene while *gauche* interactions depend on the ethyl group in the geminal position. The theoretical intensity ratios, based on the symmetry (see above) are also indicated:

(a)	$A + G_{Cs}$	intensity 1
(b)	A	intensity 1
(c)	$A + \Delta I$	intensity 2
(d)	$A + G_C + \Delta I$	intensity 2

A is the methylene chemical shift as unaffected by *gauche* contributions, while ΔI represents a further interaction to the main chain also present in PDMP. The PDMP spectrum shows a splitting of about 1 ppm, which indicates that the interaction ΔI cannot be larger than the interactions G_C and G_{Cs} in absolute value.

Starting downfield, the assignments, also based on intensity criteria, thus follow the sequence **b**:**c**:**a**:**d**. It is not surprising that the split due to the ^{31}P coupling is larger in the conformations containing G_C interactions, because the electronic configuration is affected by the conformations. This is a case in which the $^{13}C-^{31}P$ coupling constants can be accurately measured as a function of conformation.

Given the assignments, the system of four equations and four unknowns (A, G_C, G_{Cs}, ΔI) can be solved. We can thus determine the values of A (31.2 ppm), the *gauche* interaction parameters $G_C \approx G_{Cs}$ (−6 ppm), and the small contribution ΔI (−0.7 ppm). The small difference between G_{Cs} and G_C may be explained by the imprecision associated with the treatment of disorder in the case of C(14) which affects substantially the features of conformation **b** (see X-ray structure determination of TDEP). The conventional γ-*gauche* value from the literature is about −5 to −6 ppm.[32]

The methyl carbon resonances can be treated similarly, and an analogous set of equations can be written:

(a)	$B + 2G_N$	intensity 1
(b)	$B + G_{Nw} + G_{Cs}$	intensity 1
(c)	$B + G_{Ns} + G_C$	intensity 2
(d)	$B + G_{Nw} + G_N$	intensity 2

B is the methyl chemical shift as unaffected by *gauche* contributions. After substitution of the *gauche* effects resulting from the methylene spectrum, a set of four equations and four unknowns is obtained again. The assignments are less straightforward than for the methylene signals: we can, however, state that, given the similarity of the additive parameters, the signals for the **a** and **d** conformations are expected to be very close to each other, as are those for **b** and **c**. This is

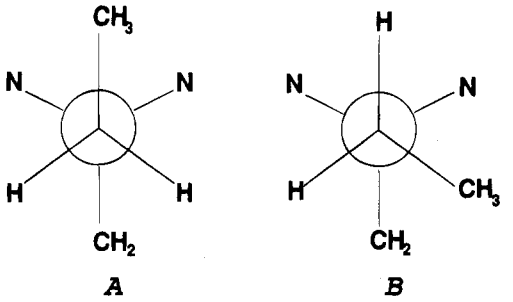

Figure 14. Newman projections, along the P–C bond, of the two conformations of the ethyl groups on the same phosphorus in TDEP.

also consistent with the intensity pattern. Thus, assignments of the signals in the order **c**:**b**:**a**:**d**, starting downfield (hypothesis I), and **d**:**a**:**b**:**c** (hypothesis II) are in principle possible. The equations were solved for both cases, producing two sets of solutions. The former set of solutions (I) does not seem to be valid since the G_N interactions do not follow a correct order from *weak* to *strong*. The resulting *gauche* effects are listed in Table 9. We believe that the *γ-gauche* effect experienced by a ^{13}C atom and due to a nitrogen has never been measured in a similar connectivity.

Dynamic Disorder in PDEP and TDEP. The chemical shifts in the spectra of the I_b and II forms of PDEP and TDEP are the results of the weighted average of the low-temperature CSs. This is a clear indication of averaging among conformations found at room temperature. Accordingly, the relaxation times of PDEP, which were already shortened by the presence of the phosphazenic ^{31}P atom, are further reduced at high temperature (Table 7). It is remarkable that, close to the transition, while the signals remain sharp, the CS range is progressively reduced with temperature for both methyls and methylenes. Moreover, the average chemical shift value is the same at the different temperatures. These observations may be interpreted in terms of an equilibrium among conformers already present before the transition.

Phase I_b is present as a minor component in the *native* samples of PDEP at room temperature and essentially pure at temperatures above the 45 °C transition. It is characterized by a high mobility of the ethyl groups on the NMR time scale. Fast interconversion among the populated conformations generates a chemical shift value corresponding to the average of the chemical shifts observed in the I_a phase. This is an indication for the occurrence of closely similar conformations as in phase I_a and of a cooperative disordering mechanism. X-ray diffraction data show a typical crystalline behavior with a pattern analogous to the phase I_a. We can therefore describe form I_b as a crystalline phase with a main-chain conformation and packing closely similar to those of phase I_a but dynamically disordered. As a consequence distinct P atoms and side chains that in I_a exist in different environments become statistically equivalent.

In some sense therefore, phase I_b can be seen as a peculiar type of mesophase with some side-chain mobility, which, however, does not disturb the *cis–trans* main-chain conformation nor the overall tridimensional order. Specifically, the X-ray data appear to rule out a hexagonal or pseudohexagonal packing typical of all the hitherto characterized polyphosphazene mesophases. In all such disordered modifications the onset of extensive side-chain motion leads to extensive disordering of the main chain and to loss of specificity in the interaction between next neighbor chains. Complete structural determinations of phases I_a and I_b would be required to characterize our structural model in more detail. As for the side-chain motions, we do not know with certainty at the moment whether they are propagating by interaction of *vicinal* positions, but this appears more probable than the assumption of uncorrelated mobility. Moreover, modeling the *geminal* ethyl conformations, a strong g^+g^- interaction was observed, similar to that proposed for the *n*-pentane molecule.[33] Totally independent motions of the *geminal* conformations are, therefore, highly unlikely. Additional evidence about the mobility will be discussed in a forthcoming article presenting solid-state ^2H NMR spectra of deuterated samples.[34]

Phase II, obtained by recrystallization, shows a NMR pattern very similar to that of phase I_b but with different T_1 values and a different X-ray diffraction pattern. The local conformational arrangement of the ethyl groups should be, therefore, similar to that described for phase I_b, while diffraction patterns show a different crystalline architecture that allows the dynamic disorder of the side chains in the range of temperatures from room temperature to the melting. Disorder involves mainly the side chains and in fact the diffraction patterns show tridimensional positional order as far as the backbone structure is concerned. The fact that phase II presents disorder features which are closely related to those of modification I_b while adopting probably the same main-chain conformation and a clearly different packing represents additional evidence of the specific and different nature of the interaction between neighboring chains in these two crystalline modifications.

The same polymorphic behavior is shown by the cyclic trimer: tentatively, we can propose that phase I_a converts, at the transition temperature, into phase I_b for which the dynamic disorder in side-chain conformation is poorly compatible with the crystal packing. Because of the intrinsically higher molecular mobility, TDEP converts, within a few degrees, to the different

Table 9. *γ-Gauche* Interactions for TDEP As Determined by NMR (ppm)[a]

	CH_3	
CH_2	hypothesis I	hypothesis II
(**b**) $A = 31.2$	(**c**) $B + G_{Ns} + G_C = 9.2$	(**d**) $B \bullet G_{Nw} + G_N = 9.2$
(**c**) $A + \Delta I = 30.5$	(**b**) $B + G_{Nw} + G_{Cs} = 8.8$	(**a**) $B + 2G_N = 8.8$
(**a**) $A + G_{Cs} = 25.3$	(**a**) $B + 2G_N = 7.0$	(**b**) $B + G_{Nw} + G_{Cs} = 7.0$
(**d**) $A + C_G + \Delta I = 24.4$	(**d**) $B + G_{Nw} + G_N = 6.5$	(**c**) $B + G_{Ns} + G_C = 6.5$
$A = 31.2$	$B = 23.6$	$B = 16.4$
$\Delta I = -0.7$	$G_{Ns} = -8.4$ (50°)	$G_{Ns} = -3.9$ (50°)
$G_{Cs} \approx C_G \approx -6$	$G_N = -8.3$ (60–65°)	$G_N = -3.8$ (60–65°)
	$G_{Nw} = -8.8$ (71°)	$G_{Nw} = -3.4$ (71°)

[a] A = unperturbed methylene chemical shift, B = unperturbed methyl. Angles were measured by X-ray diffraction.

crystalline modification II, which allows more easily dynamic disorder in side-chain conformations.

Conclusions

The resolution of the crystal structure of the ordered phase I of the cyclic trimer of diethylphosphazene allowed us to identify preferred conformational arrangements of the ethyl groups. These data, in conjunction with the NMR chemical shift values and relaxation parameters of the trimer and the polymer measured for the different crystalline modifications lead to a reasonable description of the polymorphic behavior of the trimer and the polymer.

The dynamic disordering of the ethyl side chains in the I_b and II crystalline modifications of PDEP provides an explanation of the different melting points and solubilities of PDEP and PDMP. The values of ΔS_m reported in Table 1 for the two polymers are more similar than expected; indeed the lengthening of the side chains on going from methyl to ethyl, assuming perfectly ordered crystals, should increase the melting entropy of PDEP more than the experimental 1 J/(mol K).[35] The similarity of the melting entropies of the two polymers leads to a substantially higher stability for the crystal with larger ΔH_m and can be justified only since considerably more disorder is already present in PDEP than in PDMP crystals. The high stability of PDEP crystals, and therefore the limited solubility, is due to the fact that substantial local dynamic disorder can develop in crystalline PDEP affecting the packing energy only very moderately. This corresponds only in part with what is found in most other mesomorphic polymers.

Let us conclude by noting that the surprising multiplicity of NMR signals for a single carbon may be regarded as a case of the exceptional sensitivity of MAS NMR to the molecular details in the materials. The complementarity to X-ray diffraction data, which are an essential point of reference for the often difficult interpretation of the NMR patterns in the solid state, must be noted as well.

Acknowledgment. Our thanks are due to G. G. Torri and to D. Parrilli for technical assistance. This work was supported by the "Ministero della Pubblica Istruzione" and the "Consiglio Nazionale delle Richerche".

Supplementary Material Available: Anisotropic displacement parameters and hydrogen atom positional parameters (6 pages): a list of observed and calculated structure factors for TDEP (3 pages). Ordering information is given on any current masthead page.

References and Notes

(1) Singler, R. E.; Schneider, N. S.; Hagnauer, G. L. *Polym. Eng. Sci.* **1975**, *15*, 321.
(2) Kojima, M.; Magill, J. H. *Polymer* **1989**, *30*, 579.
(3) Sun, D. C.; Magill, J. H. *Polymer* **1987**, *28*, 1243.
(4) Gomez, M. A.; Marco, C.; Fatou, J. G.; Browmer, T. N.; Haddon, R. C.; Chichester-Hicks, S. V. *Macromolecules* **1991**, *24*, 3276.
(5) Desper, C. R.; Schneider, N. S. *Macromolecules* **1976**, *9*, 424.
(6) Magill, J. H.; Riekel, C. *Makromol. Chem., Rapid Commun.* **1986**, *7*, 287.
(7) Miyata, T.; Masuko, T.; Kojima, M.; Magill, J. H. *Macromol. Chem. Phys.* **1994**, *195*, 253.
(8) Takegoshi, K.; Tanaka, I.; Hikichi, K.; Higashida, S. *Macromolecules* **1992**, *25*, 3392.
(9) Tanaka, H.; Gomez, M. A.; Tonelli, A. E.; Chichester-Hicks, S. V.; Haddon, R. C. *Macromolecules* **1988**, *21*, 2301; **1989**, *22*, 1031.
(10) Kojima, M.; Magill, J. H. *Polymer* **1985**, *26*, 1971.
(11) Kojima, M.; Magill, J. H. *Polym. Commun.* **1984**, *25*, 273.
(12) Russell, T. P.; Anderson, D. P.; Stein, R. S.; Desper, C. R.; Beres, J. J.; Schneider, N. S. *Macromolecules* **1984**, *17*, 1795.
(13) Papkov, V. S.; Il'ina, M. N.; Zhukov, V. P.; Tsvankin, D. Ja.; Tur, D. R. *Macromolecules* **1992**, *25*, 2033.
(14) Tur, D. R.; Provotorova, N. P.; Vinogradova, S. V.; Bakhmutov, V. I.; Galakhov, M. V.; Zhukov, V. P.; Dubovik, I. I.; Tsvankin, D. Ja.; Papkov, V. S. *Makromol. Chem.* **1991**, *192*, 1905.
(15) Neilson, R. H.; Hani, R.; Wisian-Neilson, P.; Meister, J. J.; Roy, A. K.; Hagnauer, G. L. *Macromolecules* **1987**, *20*, 910.
(16) Meille, S. V.; Poletti, A. R.; Gallazzi, M. C.; Gleria, M.; Brückner, S. *Polymer* **1992**, *25*, 2364.
(17) Meille, S. V.; Gallazzi, M. C.; Farina, A. *Makromol. Chem., Rapid Commun.* **1994**, *15*, 573.
(18) Kojima, M.; Magill, J. H. *Makromol. Chem.* **1992**, *193*, 2731.
(19) Wisian-Neilson, P.; Neilson, R. H. *Inorg. Synth.* **1989**, *25*, 69.
(20) Sisler, H. H.; Frarier, S. E. *Inorg. Chem.* **1965**, *4*, 1204.
(21) Bilbo, A. J. *z. Naturforsch.* **1960**, *15b*, 330.
(22) Torchia, D. A. *J. Magn. Reson.* **1978**, *30*, 613.
(23) Axelson, D. E.; Russell, K. E. *Prog. Polym. Sci.* **1985**, *11*, 221.
(24) Sheldrick, G. M. SHELXS-86: Program for the solution of crystal structures, University of Göttingen, Göttingen, Germany.
(25) Sheldrick, G. M. *J. Appl. Crystallogr.*, in preparation.
(26) Oakley, R. T.; Paddok, N. L.; Rettig, S. J.; Trotter, J. *Can. J. Chem.* **1977**, *55*, 4206.
(27) Schaefer, J.; Stejskal, E. O.; Buchdahl, R. *Macromolecules* **1977**, *10*, 384.
(28) Fukushima, E.; Roeder, S. B. *Experimental Pulse NMR: A Nuts and Bolts Approach*; Addison-Wesley: Reading, MA, 1981.
(29) VanderHart, D. L. *Makromol. Chem., Macromol. Symp.* **1990**, *34*, 125.
(30) Chatani, Y.; Yatsuyanagi, K. *Macromolecules* **1987**, *20*, 1042.
(31) Meille, S. V.; Porzio, W.; Allegra, G.; Audisio, G.; Gleria, M. *Makromol. Chem., Rapid Commun.* **1986**, *7*, 217.
(32) Tonelli, A. E. *NMR Spectroscopy and Polymer Microstructure: The Conformational Connection*; VCH Publishers: Deerfield Beach, FL, 1989.
(33) Flory, P. J. *Statistical Mechanics of Chain Molecules*; Wiley-Interscience: New York, 1969.
(34) Sozzani, P.; Simonutti, R.; Comotti, A.; Gallazzi, M. C., to be published.
(35) Wunderlich, B. *Macromolecular Physics*; Academic Press: New York, 1980; Vol. 3.

MA941119T